Cryobiology **39,** 215–227 (1999)
Article ID cryo.1999.2203, available online at http://www.idealibrary.com on IDEAL®

Effects of Solute Methoxylation on Glass-Forming Ability and Stability of Vitrification Solutions

Brian Wowk,[1] Michael Darwin, Steven B. Harris, Sandra R. Russell, and Christopher M. Rasch

21st Century Medicine, Inc., 10844 Edison Court, Rancho Cucamonga, California 91730, U.S.A.

The effects of replacing hydroxyl groups with methoxyl (OCH_3) groups in the polyols ethylene glycol (EG), propylene glycol (PG), glycerol, and threitol were studied by differential scanning calorimetry (DSC) during cooling of aqueous solutions to −150°C and subsequent rewarming. For 35% (w/w) PG, 40% EG, and 45% glycerol, a single substitution of a terminal hydroxyl group with a methoxyl group reduced the critical cooling rate necessary to avoid ice on cooling (vitrify) from approximately 500 to 50°C/min. This reduction was approximately equivalent to increasing the parent polyol concentration by 5% (w/w). The critical warming rate calculated to avoid formation of ice on rewarming (devitrification) was also reduced by methoxyl substitution, typically by a factor of 10^4 for dilute solutions. Double methoxylation (replacement of both terminal hydroxyls) tended to result in hydrate formation, making these compounds less interesting. An exception was threitol, for which substituting both terminal hydroxyls by methoxyls reduced the critical rewarming rate of a 50% solution by a factor of 10^7 without any hydrate formation. These glass-forming and stability properties of methoxylated compounds, combined with their low viscosity, enhanced permeability, and high glass transition temperatures, make them interesting candidate cryoprotective agents for cryopreservation by vitrification or freezing.

Key Words: methoxylation; cryoprotectant; vitrification; calorimetry; phase diagram; hydrates.

Numerous small molecules are known to exhibit cryoprotective effects (17), yet the search continues (2, 5, 10, 13, 14) for novel penetrating agents that may be useful in freezing and vitrification (13–15) solutions. In particular, there is a need for cryoprotectants with reduced viscosity for applications involving organ perfusion (12). There is also a need for cryoprotectants that penetrate rapidly for use with systems resistant to penetration by conventional cryoprotectants (16). Vitrification also requires that agents readily form glasses that remain stable during rewarming at rates that are practically achievable.

We have explored the strategy of modifying conventional polyol cryoprotectants by substituting methoxyl (—OCH_3) groups for hydroxyl (—OH) groups on cryoprotectant molecules. Hydroxyl groups can hydrogen bond to either water molecules or hydroxyl groups on other cryoprotectant molecules. Therefore, cryoprotectants that contain hydroxyl groups "waste" a significant portion of their water interaction capacity by interacting with adjacent cryoprotectant molecules instead of water. Unlike hydroxyl groups, the ether linkages of methoxyl groups interact minimally with other ether groups. Yet the ether linkage can still hydrogen bond to water. Methoxylated cryoprotectants are therefore expected to exhibit reduced self-interaction and enhanced water interaction compared to their conventional polyol analogs. This enhanced water binding efficiency might be expected to materially influence the glass-forming properties of these molecules in solution.

Table 1 shows families of methoxylated cryoprotectants formed by starting with four basic polyols (ethylene glycol, propylene glycol, glycerol, and threitol) and substituting either one or two hydroxyl groups with methoxyl groups. Table 2 shows that methoxylated compounds exhibit reduced viscosity (as pure

Received June 4, 1999; accepted August 23, 1999.

Funding for this study was provided by 21st Century Medicine, Inc.

[1] To whom correspondence should be addressed. Fax: (909) 466-8618. E-mail: wowk@21cm.com.

0011-2240/99 $30.00

TABLE 1
Solutes Studied

Abbreviation	Common name	Systematic name	Methoxyl substitutions
EG	Ethylene glycol	1,2-Ethanediol	0
EGMME	Ethylene glycol monomethyl ether	2-Methoxyethanol	1
EGDME	Ethylene glycol dimethyl ether	1,2-Dimethoxyethane	2
PG	Propylene glycol	1,2-Propanediol	0
PGMME	Propylene glycol monomethyl ether	1-Methoxy-2-propanol	1
Glycerol	Glycerol	1,2,3-Propanetriol	0
GMME	1-*O*-Methyl-rac-glycerol	3-Methoxy-1,2-propanediol	1
GDME	1,3-Di-*O*-methyl-glycerol	1,3-Dimethoxy-2-propanol	2
Threitol	DL-Threitol	1,4-Dihydroxy-DL-2,3-butanediol	0
TDME	1,4-Di-*O*-methyl-DL-threitol	1,4-Dimethoxy-DL-2,3-butanediol	2

agents) and enhanced penetration of red blood cells in aqueous solution. Enhanced penetration is due in part to the greater partitioning (k_{ether}) of methoxylated compounds into the lipid phase of cell membranes.

Methoxylated compounds have appeared previously in the cryobiological literature. Ethers of diethylene glycol have been used to freeze red cells (33). EGMME has been used to successfully freeze embryos (31, 32), oocytes (30), and spinach thylakoids (25). GMME has been used to freeze monocytes with a higher recovery rate than glycerol (26). Notably, GMME was also observed to penetrate monocytes more than six times faster than glycerol. Preliminary toxicity studies (24) of methoxylated compounds as components of vitrification solutions have been encouraging, especially for GMME and EGMME.

The objective of this study was to evaluate the glass-forming properties of methoxylated compounds as monoagents in aqueous solution. Calorimetric data for both cooling and rewarming at rates between 5 and 80°C/min were obtained. It is anticipated that this information will be useful for understanding the behavior of methoxylated compounds in solutions used for freezing or vitrification. These results have been previously presented in preliminary form (34).

TABLE 2
Viscosity, Permeability, and Ether:Water Partition Coefficient (k_{ether}) for Various Solutes

Agent	Viscosity (cP)	Red blood cell permeability	k_{ether}
EG	25.0	3.4	0.0053
EGMME	1.7	12.0	0.061
EGDME	0.5	—	—
PG	60	1.8	0.018
PGMME[a]	2	—	—
Glycerol	1400	0.6	0.00066
GMME[a]	45	1.0	0.019
GDME[a]	3	—	—

Note. Viscosities of pure solutes at 20 to 25°C from Ref. (11). Permeability and k_{ether} data from Ref. (23). Permeabilities are relative to water = 915.

[a] Viscosities not available in Ref. (11). Viscosities were instead measured by falling-ball viscosimeter at 22°C.

MATERIALS AND METHODS

Solutes were obtained from Aldrich Chemical Company in HPLC, spectrophotometric, or ACS reagent grades. GMME was obtained from Sigma Chemical Company. TDME was obtained from Fluka. GDME was custom synthesized by Drs. John Bender and Fred West of the Department of Chemistry, University of Utah, Salt Lake City, Utah, U.S.A. Solutions were prepared in distilled water (Hinckley & Schmitt,

Inc.) on a gravimetric basis. Even if not stated explicitly, solution concentrations are always given as weight-by-weight (w/w) percent.

Cooling and rewarming thermograms were obtained with a Perkin–Elmer DSC 7 differential scanning calorimeter running Pyris version 2.04 software. Solution samples of mass from 5 to 15 mg were sealed in Perkin–Elmer 0219-0062 aluminum sample pans and placed in the DSC sample oven for analysis. An empty sample pan was kept in the DSC reference oven to balance the instrument. The oven temperature was calibrated by measuring the onset of the crystal transition of cyclohexane at −87.06°C while warming at 1°C/min and the onset of melting of water ice at 0°C. Heat flow was calibrated by measuring the area under the melting curve of a known mass of water ice (334 J/g nominal).

Cooling thermograms were obtained during scanning from +10 to −150°C at rates of 5, 10, 20, 40, and 80°C/min. To account for sample-to-sample variability observed during cooling experiments, thermograms were obtained for three different samples of each solute concentration. Quantities of ice crystallized were measured as the parameter q, defined by Boutron (3–10) as the percentage ratio of heat liberated during freezing to the heat that would be liberated if a mass of water equal to the entire solution mass were frozen at 0°C. It is approximately equal to the mass percentage of the solution that converts to ice.

The mean value of q was plotted for each solute concentration as a function of cooling rate, and a least-squares fit to the fourth model of Boutron (3, 10) was performed. In this model, the quantity of ice formed on cooling follows the relation

$$\frac{k_4}{|v|} = -\ln(1 - x^{1/3}) + \frac{1}{2}\ln(1 + x^{1/3} + x^{2/3}) + \sqrt{3}\arctan\left(\frac{\sqrt{3}x^{1/3}}{2 + x^{1/3}}\right),$$

where $x = q/q_{\max}$ ($0 \le x \le 1$) is the ratio of ice crystallized on cooling to the maximum quantity of ice that crystallizes during very slow cooling ($q_{\max}$), v is the cooling rate, and k_4 is a constant. k_4 and $q_{\max}$ are the free parameters of the least-squares fit to the measured data. Theoretical critical cooling rates v_{thcrc} were calculated from (2, 4)

$$v_{\text{thcrc}} = \frac{k_4}{3 \times \left(\frac{0.2}{q_{\max}}\right)^{1/3}}.$$

This is the cooling rate at which the quantity of ice formed on cooling becomes negligible (q = 0.2), corresponding to approximately 0.2% of the solution mass freezing.

To determine stability of the vitreous state, thermograms were obtained during rewarming of vitrified samples from −150 to +10°C at rates of 5, 10, 20, 40, and 80°C/min. Prior to warming, samples were first "quenched" by cooling from ambient temperature to −150°C at a rate of 100°C/min. The DSC was able to maintain this nominal rate in all cases until approximately −120°C, below which the sample temperature slightly lagged the programmed cooling rate. Warming runs were usually not performed on samples which did not vitrify during cooling at 100°C/min. However, warming thermograms were obtained for some samples that formed hydrates on cooling. Typically only one warming thermogram at a given warming rate was performed for each solute concentration because the variability of the warming data was very small.

Warming thermograms were analyzed to obtain the glass transition temperature T_g, ice devitrification temperature T_d, and ice melting temperature T_m. The glass transition temperature T_g was defined as the inflection point of the rapid change of specific heat at the glass transition (4–8). T_d and T_m were defined as the peaks of the ice devitrification and melting peaks, respectively (4–8).

$T_m - T_d$ was plotted as a function of the logarithm of the warming rate, and a linear fit to the resulting plot was performed (4–7). More recent work (9, 18, 20–22) suggests that the plot of T_m/T_d vs log warming rate may be more

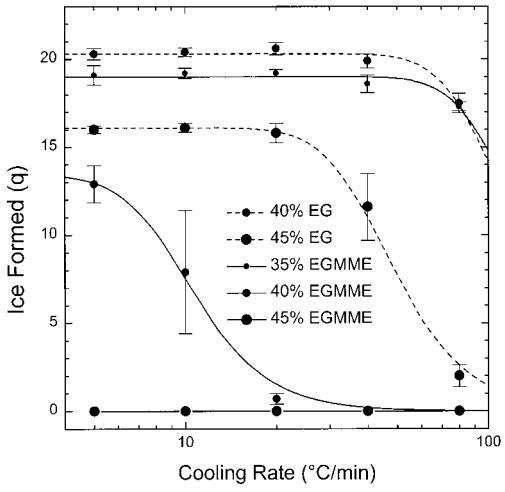

FIG. 1. Quantity of ice crystallized (q) vs cooling rate for EG and EGMME solutions. Each data point is the mean of three samples. Error bars are the sample standard deviation. Fitted curves correspond to the fourth model of Boutron (3). Hydrate forms in the EGMME solutions when the amount of ice formed becomes small.

appropriate. However, we choose to plot $T_m - T_d$ to facilitate comparison to previously published data. $T_m - T_d$ also has the advantage that temperature lag effects caused by finite sample mass at high heating rates are implicitly subtracted out.

Critical rewarming rates v_{crr} (rewarming rates necessary to avoid devitrification) were calculated according to Eq. [14] of the model of Boutron (9), which extrapolates the linear variation of T_m/T_d vs log warming rate to $T_d/T_m = 0.95$, corresponding to approximately $q_{dm} = 0.5$ or 0.5% of the solution devitrifying to ice on rewarming. Input values of T_d for this model were computed by first fitting a line to the T_m - T_d data plots and using the fitted line to calculate T_d at 5 and 80°C/min.

RESULTS

EG Derivatives

EGMME was investigated. The quantity of ice formed on cooling as a function of cooling rate is shown in Fig. 1 for EG and EGMME. The calculated critical cooling rates and related parameters are in Table 3. A solution of 35% EGMME froze with no hydrate formation for all cooling rates studied. With 40% EGMME, the quantity of ice formed decreased rapidly as cooling rate increased, reaching zero for cooling rates ≥40°C/min. However, as the amount of ice decreased, a hydrate peak at −87°C became increasingly apparent (Fig. 2). No ice formed on cooling solutions of 45% concentration or greater. Instead an apparent hydrate formed at −86, −87, −90, and −93°C for 45, 50, 55, and 60% concentrations, respectively. At 70% concentration, the hydrate formation could be avoided by cooling at 80°C/min or greater. At still higher concentrations, a glass transition always occurred instead of hydrate formation.

Figure 3 shows thermograms obtained during slow rewarming of quenched EGMME solutions. Figure 4 shows the associated dynamic phase diagram. None of the samples formed ice on cooling; however, samples of less than 70% concentration formed hydrate during cooling.

There is evidence for two distinct forms of hydrate in EGMME solutions. Both appeared near −90°C on cooling. The first hydrate occurred during cooling solutions of 45% or lower concentration (if little or no ice formed first) and appeared in bulk solutions as a chalky white solid. On warming, this hydrate melted isothermally at −82°C and was followed by an ice melt (Fig. 3). Ice apparently crystallizes together with this hydrate because the ice melt was not preceded by ice devitrification. The second hydrate occurred in solutions of 50 to 70% concentration. In bulk solutions, it appeared as a mild fog throughout the mostly transparent solution. On warming, this hydrate melted nonisothermally near −75°C and was followed by ice devitrification and melting in the 50% solution.

EGDME was also investigated. The behavior of this solute was complicated. On cooling 35% solutions, three sharp solidification peaks appeared at −44, −63, and −106°C. The same peaks appeared while cooling 40% solutions at 20°C/min or less. At faster cooling rates the 40% solution vitrified. Solutions of 45 and 50% vitrified at all cooling rates tested.

The dynamic phase diagram obtained by slow rewarming EGDME samples is shown in

TABLE 3
Transition Temperatures (°C), Crystallization Constants, Critical Cooling (v_{thcrc}), and Critical Warming (v_{crr}) Rates in °C/Minute for Solutes Tested

Solution (w/w)	T_g	T_d	T_m	q_{max}	k_4	v_{thcrc}	v_{crr}
40% EG				20.3	348	541	
45% EG	−131	−110	−30	16.1	137	197	8×10^5
50% EG	−129	−87	−38			<5	250
35% EGMME				19.0	386	587[a]	
40% EGMME			−25	13.4	30	41[a]	
45% EGMME			−30			<5[a]	
50% EGMME			−37			<5[a]	80[a]
40% EGDME	−103		−21			40	
45% EGDME	−103		−28			<5	200
50% EGDME	−107					<5	5
35% PG	−119[b]	−104[b]	−18[b]	21.2	352	555	2×10^7
40% PG	−108[b]	−87[b]	−22[b]	17.1	49	72	$1.0 \times 10^{4\,b}$
45% PG	−107	−58	−27			<5	160
35% PGMME	−105	−84	−16	19.9	35	54	7×10^3
40% PGMME	−102	−65	−20			<5	650
45% PGMME	−101	−58	−27			<5	290
50% PGMME	−101	−55	−29			<5	80
45% glycerol	−117	−108	−20	21.9	291	464	$5.6 \times 10^{8\,b}$
50% glycerol	−115	−98	−24	18.0	54	81	1×10^6
40% GMME				20.7	360	560	
45% GMME	−103	−89	−21	19.9	15	23	4×10^4
50% GMME	−101	−67	−26			<5	350
55% GMME	−99	−61	−32			<5	80
60% GMME	−99	−59	−40			<5	10
40% GDME			−17	19.4	75	115[a]	
45% GDME	−94		−21	19.0	13	20[a]	
50% GDME	−95		−27			<5	
55% GDME	−98		−32			<5	80
60% GDME	−98		−35			<5	10
50% threitol	−106	−98	−18			≈100[c]	2×10^9
60% threitol	−98	−53	−28			<5	80
50% TDME	−84	−58	−23			<5	280
60% TDME	−85		−34			<5	20

Note. Transition temperatures were measured during warming at 5°C/min. q_{max} and k_4 were computed according to the fourth model of Boutron (3). v_{thcrc} and v_{crr} were computed according to Refs. (4) and (9), respectively. Values of $v_{crr} < 200$ were determined by direct observation, not calculation.

[a] Ice is avoided, but hydrate still forms.

[b] From Refs. (6, 9).

[c] Determined by direct observation, not calculation.

Fig. 5. The hydrate devitrification and melting events seen in the 45% solution disappeared at warming rates of 20°C/min or greater, replaced by only ice devitrification and melting peaks. The critical rewarming rate, v_{crr}, to avoid devitrification of the 45% solution was calculated to be approximately 200°C/min. A 50% solution of EGDME was found to be stable (no ice or

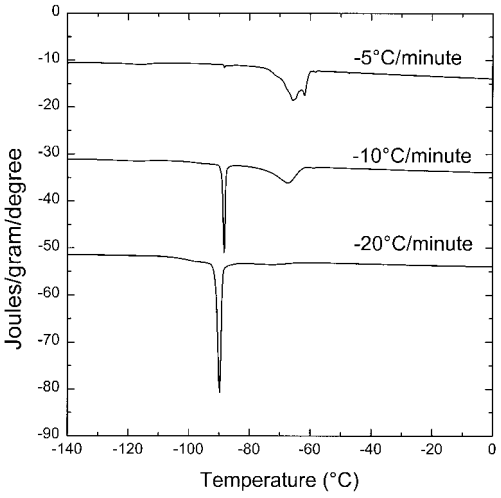

FIG. 2. Cooling thermograms for 40% EGMME solution cooled at various rates. The hydrate near −90°C only appears at higher cooling rates that do not allow ice to crystallize first.

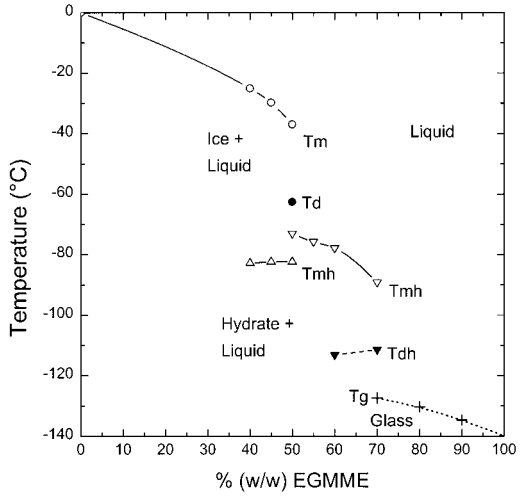

FIG. 4. Dynamic phase diagram for EGMME obtained by rewarming rapidly cooled solutions at +5°/min. T_m denotes the ice melting temperature, T_d ice devitrification temperature, T_g glass transition temperature, T_{dh} hydrate devitrification temperature, and T_{mh} hydrate melting temperature. Two distinct hydrate melting curves are apparent, although they are both denoted by T_{mh}.

hydrate formation) at all cooling and warming rates tested. At higher concentrations, hydrates appeared again. Near 100% concentration a single peak remained, coinciding with the literature value (11) for the melting point of pure EGDME.

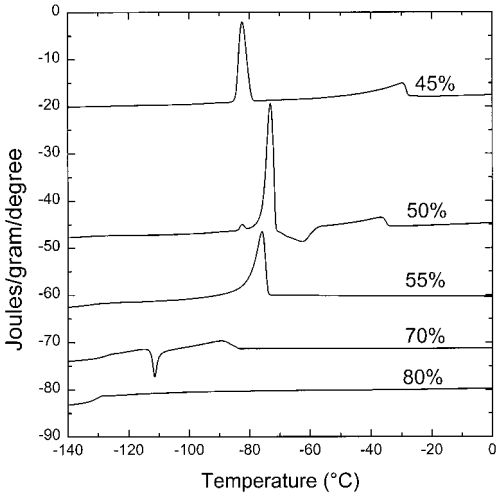

FIG. 3. Warming thermograms at +5°C/min for various concentrations (w/w) of EGMME. The 45% thermogram shows a hydrate melt and ice melt. The 50% thermogram shows two hydrate melting peaks, ice devitrification, and ice melting. The 55% thermogram shows only a nonisothermal hydrate melt. 70% shows hydrate devitrification and melting. 80% shows only a glass transition.

PG Derivatives

PGMME behaved like a conventional cryoprotectant on both cooling and rewarming. There were no hydrates or other unusual thermographic features. The quantity of ice formed on cooling is shown in Fig. 6 for PG and PGMME. PGMME is clearly a better glass former than PG, though not quite as good as meso-depleted 2,3-butanediol (4, 5).

It should be noted that the values of k_4 and the associated critical cooling rates measured for PG were approximately twice as large as those measured by Boutron (4, 7) and thrice as large as those measured by Sutton (27). Perhaps this was due to a purity difference in the PG we used (Aldrich 39,803-9, ACS reagent grade). In contrast, our measurements with EG and glycerol agree reasonably well with previous results obtained by Boutron (6, 8, 9). Our glycerol results also agree very well with the critical

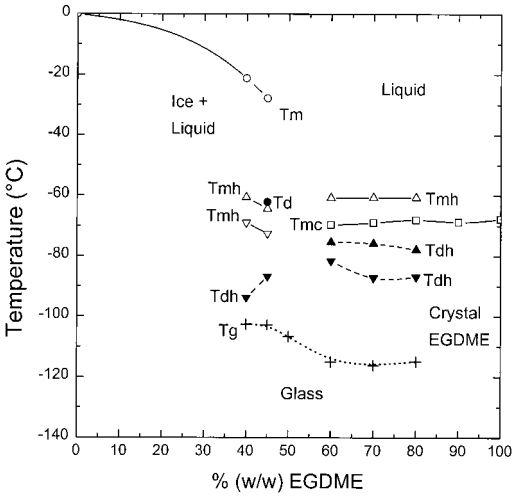

FIG. 5. Dynamic phase diagram for EGDME obtained by rewarming rapidly cooled solutions at +5°/min. Same comments apply as for Fig. 4. T_{mc} denotes the melting temperature of pure crystalline EGDME. The phase behavior of EGDME is complex except for a narrow concentration regime near 50% where only a glass transition occurs.

cooling rates that Sutton (28, 29) determined by isothermal emulsion calorimetry.

Slow rewarming thermograms for PGMME solutions are shown in Fig. 7 and the associated dynamic phase diagram in Fig. 8. The calculated critical rewarming rates in Table 3 and the variation of $T_m - T_d$ with warming rate in Fig. 9 show that dilute solutions of PGMME are much more stable on rewarming than compara-

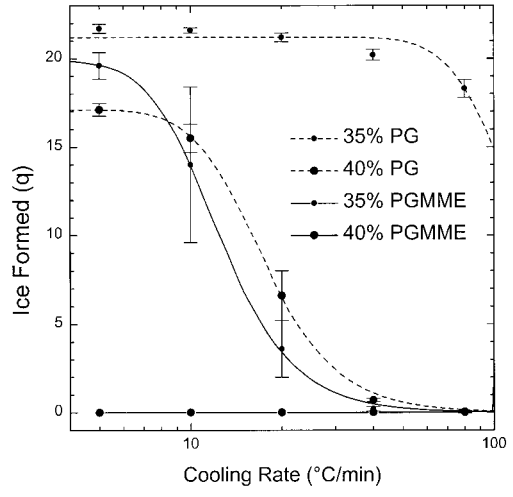

FIG. 6. Quantity of ice crystallized (q) vs cooling rate for PG and PGMME solutions. The same comments apply as for Fig. 1.

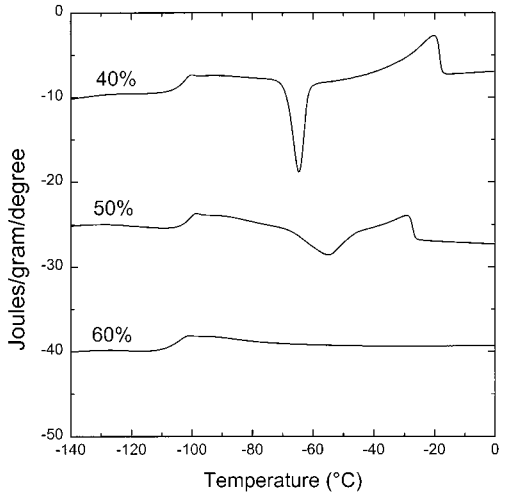

FIG. 7. Warming thermograms at +5°C/min for various concentrations (w/w) of PGMME. The only apparent events are the glass transition, ice devitrification, and ice melting peaks. Only a glass transition occurs at 60% concentration.

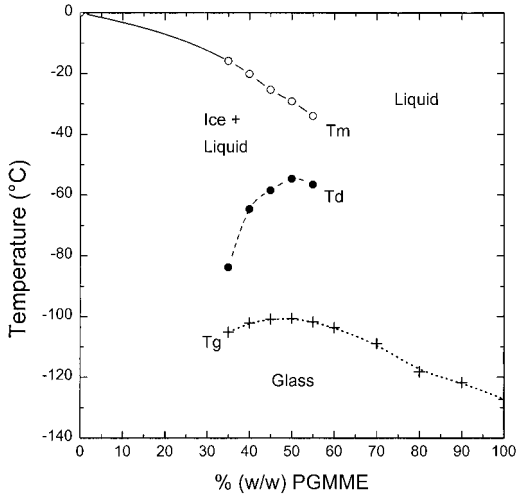

FIG. 8. Dynamic phase diagram for PGMME obtained by rewarming rapidly cooled solutions at +5°/min. Same comments apply as for Fig. 4. The phase behavior of PGMME is that of a typical cryoprotectant, except for the appearance of a maximum in the glass transition temperature curve.

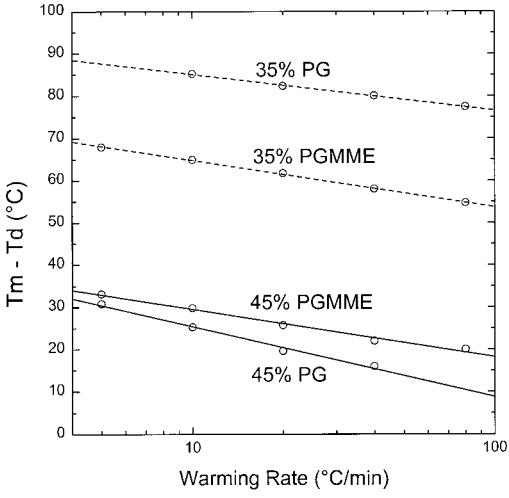

FIG. 9. $T_m - T_d$ vs warming rate for vitrified PG and PGMME solutions rewarmed from −150°C. T_d is the ice devitrification temperature and T_m is the ice melting temperature. PGMME is more stable (smaller $T_m - T_d$) against devitrification during rewarming than PG at 35% concentration, but performs similar to PG at 45% concentration.

ble PG solutions. However, the stability advantage disappears at 45% concentration. Interestingly, the glass transition temperature for PGMME solutions reaches a maximum at 50% concentration. This is an unusual behavior that previously has only been observed for solutions of diethylformamide (2).

1,2-Dimethoxypropanol (PG with both hydroxyls replaced with methoxyls) was also investigated, but was found to be poorly soluble in water.

Glycerol Derivatives

GMME also behaved like a conventional cryoprotectant on both cooling and rewarming. The quantity of ice formed on cooling is shown in Fig. 10a for glycerol and Fig. 10b for GMME. The critical cooling rates (Table 3) computed for 45% glycerol, 45% EG, and 45% GMME were 464, 197, and 23°C/min, respectively. Thus GMME appears to be a better glass former than either glycerol or EG.

GMME rewarming thermograms and dynamic phase diagram are shown in Figs. 11 and 12, respectively. $T_m - T_d$ variation with warming rate is plotted in Fig. 13. GMME was more stable on rewarming than glycerol, with a stability similar to EG.

GDME cooling thermograms are shown in Fig. 14 and quantities of ice formed in are shown in Fig. 10c. GDME behaved similarly to EGMME in that a hydrate tended to form on cooling (solidification peak at −82°C for a 45% solution cooled at 5°C/min). The hydrate was suppressed if a large quantity of ice solidified during cooling. However, unlike EGMME, a cooling hydrate did not occur in solutions of 50% concentration or greater. These solutions simply transitioned to a vitreous state on cooling.

GDME warming thermograms and the associated dynamic phase diagram are shown in Figs. 15 and 16, respectively. A hydrate devitrification and melt followed by an ice devitrification and melt are observed. The hydrate and ice solidification events disappeared together at rewarming rates of 80°C/min in 55% solutions and 10°C/min in 60% solutions.

Threitol Derivatives

TDME, which is DL-threitol with the terminal hydroxyls replaced by methoxyls, was investigated. A solution of 50% TDME vitrified with no ice or hydrate formation at all cooling rates studied, whereas the critical cooling rate of 50% threitol was approximately 100°C/min. Lower concentrations of TDME were not studied due to the expense of the material. Also for this reason, TDME solutions could only be prepared to a concentration accuracy of ±1%.

TDME was much more stable than threitol on rewarming (Fig. 17 and Table 3), with a critical warming rate similar to ethylene glycol. No hydrates were observed during rewarming.

It should also be noted that no hydrates were observed to form in solutions of the parent compound, threitol. This is unlike the behavior of erythritol (meso isomer of threitol), which in water solution has been observed to form a solid of unknown nature during cooling (10).

DISCUSSION

For 35% PG, 40% EG, and 45% glycerol, a single substitution of a terminal hydroxyl group

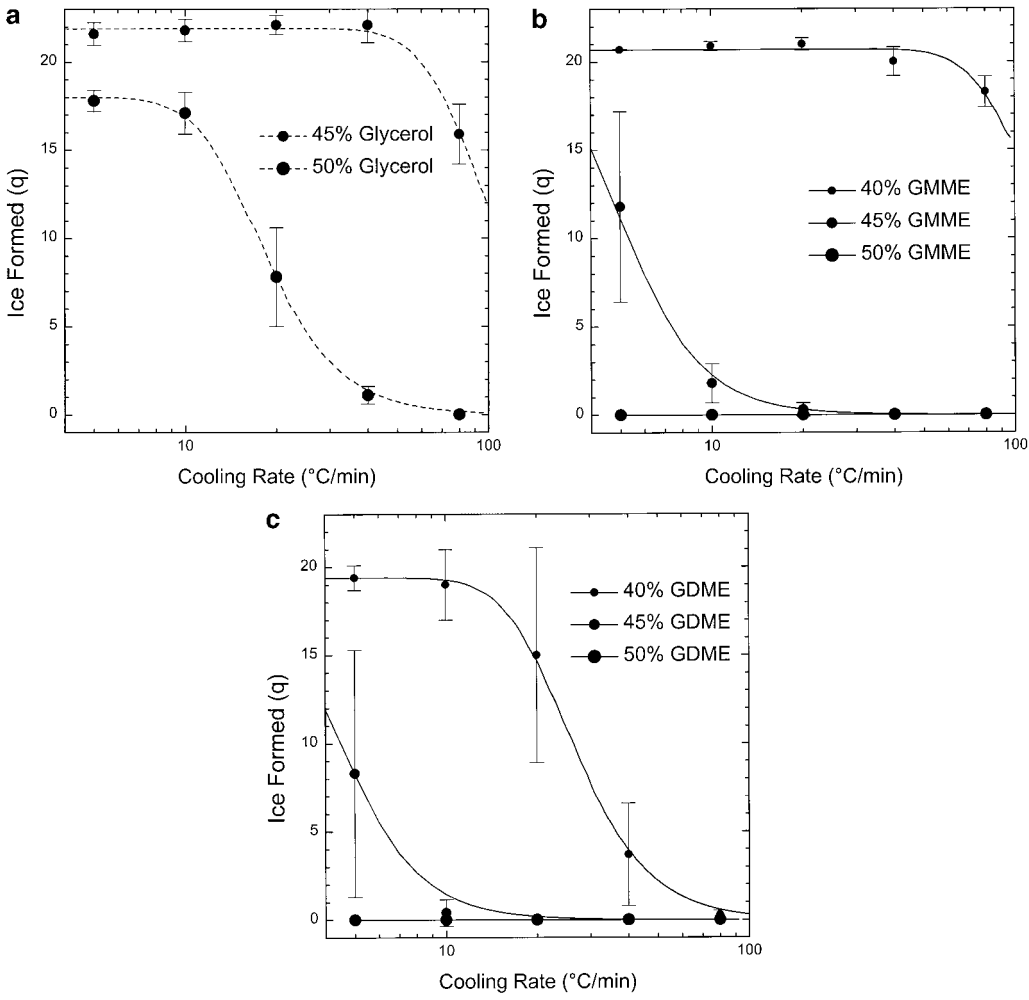

FIG. 10. (a) Quantity of ice crystallized (q) vs cooling rate for glycerol solutions. (b) Quantity of ice crystallized (q) vs cooling rate for GMME solutions. (c) Quantity of ice crystallized (q) vs cooling rate for GDME solutions. Hydrate forms in the 40 and 45% solutions at high cooling rates, but not in the 50% solution. The same comments apply as for Fig. 1.

with a methoxyl group reduced the critical cooling rate from approximately 500 to 50°C/min. For 40% PG, 45% EG, 50% glycerol, and 50% threitol, single methoxylation reduced the critical cooling rate from approximately 100°C/min. to less than 5°C/min. Methoxylating a polyol cryoprotectant thus reduces the critical cooling rate by an order of magnitude or allows the cryoprotectant concentration required for vitrification at a given cooling rate to be reduced by more than 5%. Although this analysis neglects the presence of the hydrate in the case of methoxylated EG (EGMME), the trend is still clear.

Methoxylation also improved stability of the vitreous state on rewarming, sometimes dramatically. Methoxyl substituting the terminal hydroxyls of threitol reduced the critical rewarming rate of a 50% solution by seven orders of magnitude. In some cases, particularly PG vs PGMME, the stability benefit was greatest in dilute solutions. This may be because at higher

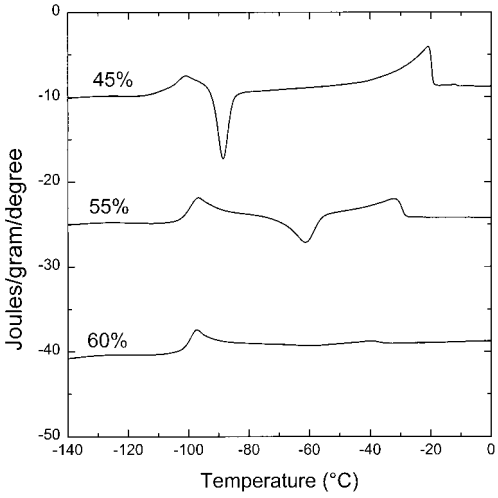

FIG. 11. Warming thermograms at +5°C/min for various concentrations (w/w) of GMME. The only apparent events are a large glass transition, ice devitrification, and ice melting peaks.

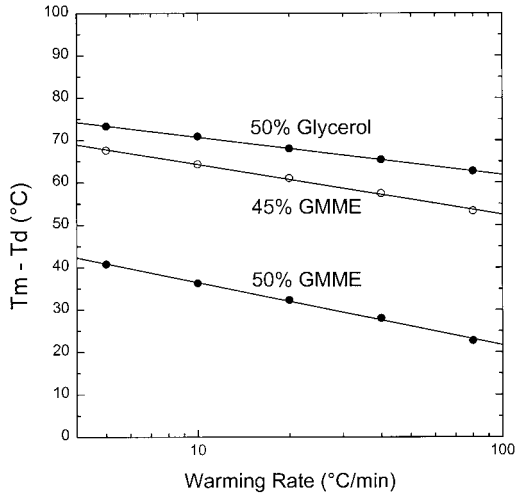

FIG. 13. $T_m - T_d$ vs warming rate for vitrified glycerol and GMME solutions rewarmed from −150°C. GMME is much more stable against devitrification than glycerol at the same concentration.

concentrations the viscosity difference between the two solutions becomes larger, allowing the greater viscosity of the PG solution to exert a stronger inhibition of ice growth.

The data of Table 3 suggest that double methoxylation does not give large reductions of critical cooling or warming rates compared to

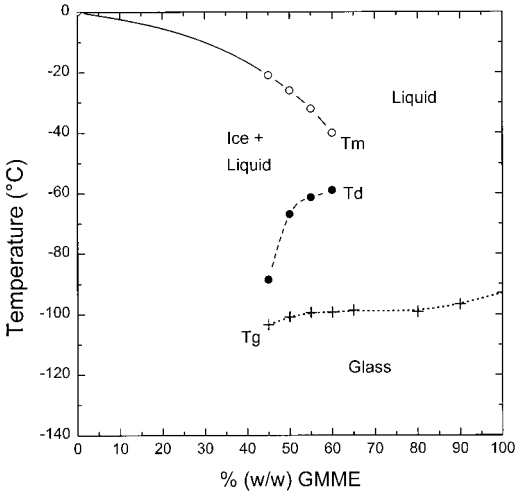

FIG. 12. Dynamic phase diagram for GMME obtained by rewarming rapidly cooled solutions at +5°/min. Same comments apply as for Fig. 4. The phase behavior of GMME is that of a typical cryoprotectant.

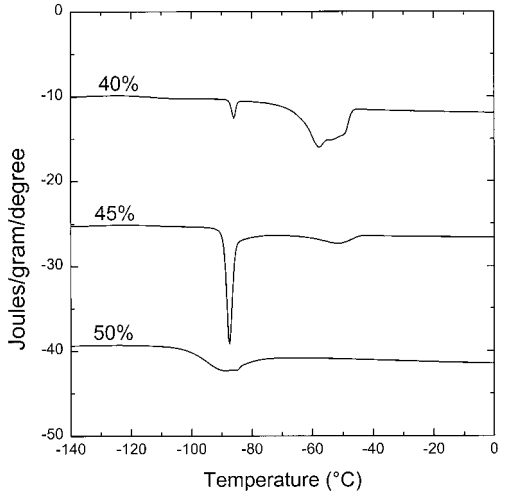

FIG. 14. Cooling thermograms obtained at −20°C/min cooling rate for various concentrations (w/w) of GDME. At lower concentrations, the hydrate solidification is suppressed by the crystallization of ice (which freeze concentrates the remaining solution into the regime where hydrate formation does not occur). At 50% concentration and above, only a large glass transition occurs on cooling.

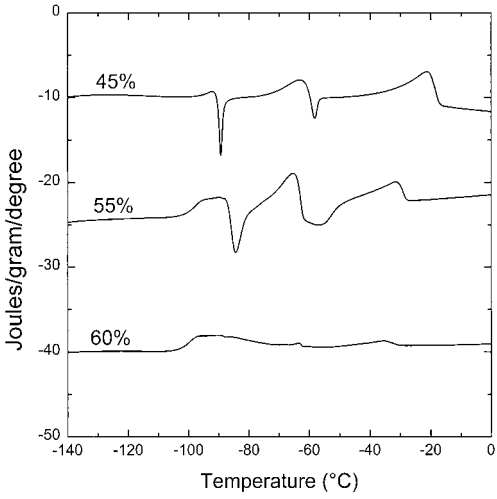

FIG. 15. Warming thermograms at +5°C/min for various concentrations (w/w) of GDME. The glass transition is followed by a rapid hydrate devitrification, hydrate melt, and then ice devitrification and ice melt. At 60% concentration, hydrate and ice melting peaks are barely visible.

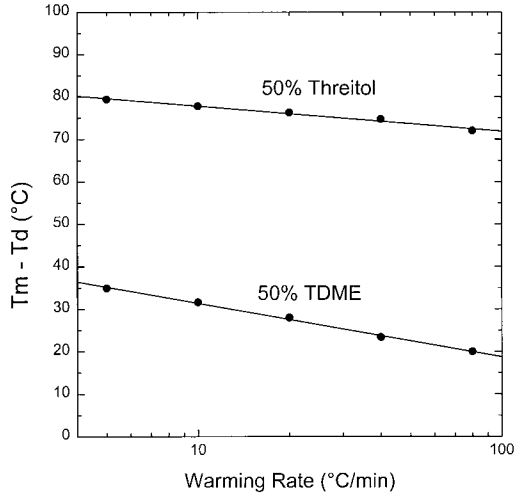

FIG. 17. $T_m - T_d$ vs warming rate for vitrified threitol and TDME solutions rewarmed from −150°C. TDME is much more stable against devitrification than threitol of the same concentration.

single methoxylation alone. The critical warming rate of EGMME vs EGDME is the only exception. Double methoxylation further reduces viscosity and enhances cell penetration; however, this must be balanced against the greater partitioning into lipids (hydrophobicity) that is correlated with toxicity to cell membranes (1).

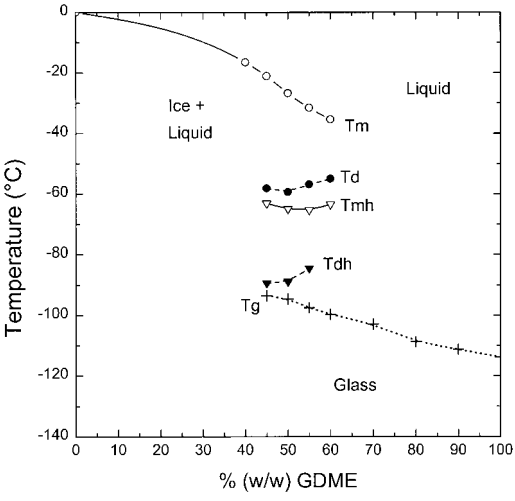

FIG. 16. Dynamic phase diagram for GDME obtained by rewarming rapidly cooled solutions at +5°/min. Same comments apply as for Fig. 4. The phase diagram of GDME is that of a typical cryoprotectant, except for the hydrate devitrification and melting before the ice devitrification and melting events.

Table 4 is a summary of glass transition temperatures measured during slow rewarming from the vitreous state. Despite the reduced viscosity of methoxylated compounds at ambient temperature, the glass transition temperature of their solutions is generally higher than that of conventional cryoprotectants. This property of methoxylated compounds could have important benefits for increasing the temperature at which cryopreserved materials must be stored and shipped. Perhaps novel penetrating agents or combinations of agents could be developed that glass transitioned above the sublimation temperature of dry ice (−78°C).

Some of the methoxylated compounds, notably GMME, GDME, and TDME, exhibited a glass transition with an anomalous peak. Similar behavior has been noted with PG (7) and especially 1,2-butanediol (10). Such peaks may be associated with a microphase separation of the solute and solvent near the glass transition that is not optically visible (19).

TABLE 4
Glass Transition Temperature (°C) vs Solute Concentration (w/w)

Agent	35%	40%	45%	50%	55%	60%	70%	80%	90%	100%
EG		−133[a]	−131	−129						
EGMME							−127	−130	−135	−140
EGDME		−103	−103	−103	−107	−115	−116	−115		
PG	−118[b]	−108[b]	−107[b]	−106[b]		−107[b]	−110[b]	−109[b]	−108[b]	−104[b]
PGMME	−105	−102	−101	−101	−102	−104	−109	−118	−122	−127
Glycerol			−117	−115						
GMME			−103	−101	−99	−99		−99	−97	−93
GDME			−94	−95	−98	−100		−109	−111	−114
Threitol				−106		−98				
TDME				−84		−85				

Note. Glass transition temperatures observed during rewarming at 5°C/min.
[a] Linear extrapolation of values obtained at 45 and 50%.
[b] Values from Ref. (7).

CONCLUSION

Replacing terminal hydroxyl groups of polyol cryoprotectants with methoxyl groups reduces the viscosity, increases the permeability, and increases the glass-forming tendency of cryoprotectant solutions. Monomethoxyl-substituted compounds vitrified and showed stability against devitrification similar to solutions of the parent compound at 5% greater concentration. The glass transition temperature was also increased. Double methoxyl substitution further increased the glass transition temperature, but provided little additional glass forming benefit for EG- and glycerol-derived compounds.

GMME, PGMME, and TDME are perhaps the most promising methoxylated compounds studied because they were not observed to form hydrates under any conditions. EGMME may also be useful for applications requiring very high permeability agents and in which the hydrates can be tolerated or avoided.

ACKNOWLEDGMENTS

We thank Dr. John Bender and Dr. Fred West of the Department of Chemistry, University of Utah, for the synthesis of 1,3-dimethoxy-2-propanol. We also thank Dr. Gregory Fahy for a critical reading of the manuscript. Finally, we thank Mr. Douglas Skrecky for bringing the paper by Naccache and Sha'afi to our attention, which stimulated our thinking in the direction of novel cryoprotectants.

REFERENCES

1. Bakaltcheva, I. B., Odeyale, C. O., and Spargo, B. J. Effects of alkanols, alkanediols and glycerol on red blood cell shape and hemolysis. *Biochim. Biophys. Acta* **1280,** 73–80 (1996).
2. Baudot, A., and Boutron, P. Glass-forming tendency and stability of aqueous solutions of diethylformamide and dimethylformamide. *Cryobiology* **37,** 187–199 (1998).
3. Boutron, P. Comparison with the theory of the kinetics and extent of ice crystallization and of the glass-forming tendency in aqueous cryoprotective solutions. *Cryobiology* **23,** 88–102 (1986).
4. Boutron, P. glass-forming tendency and stability of the amorphous state in solutions of a 2,3-butanediol containing mainly the levo and dextro isomers in water, buffer, and Euro-Collins. *Cryobiology* **30,** 86–97 (1993).
5. Boutron, P. Levo- and dextro-2,3-butanediol and their racemic mixture: Very efficient solutes for vitrification. *Cryobiology* **27,** 55–69 (1990).
6. Boutron, P., and Kaufmann A. Stability of the amorphous state in the system water–glycerol–ethylene glycol. *Cryobiology* **16,** 83–89 (1979).
7. Boutron, P., and Kaufmann A. Stability of the amorphous state in the system water–1,2-propanediol. *Cryobiology* **16,** 557–568 (1979).
8. Boutron, P., Kaufmann, A., and Van Dang, N. Maximum in the stability of the amorphous state in the system water–glycerol–ethanol. *Cryobiology* **16,** 372–389 (1979).
9. Boutron, P., and Mehl, P. Theoretical prediction of devitrification tendency: Determination of critical

warming rates without using finite expansions. *Cryobiology* **27,** 359–377 (1990).
10. Boutron, P., Mehl, P., Kaufmann, A., and Augibaud, P. Glass forming tendency and stability of the amorphous state in aqueous solutions of polyalcohols with four carbons. I. Binary systems water-polyalcohols. *Cryobiology* **23,** 453–469 (1986).
11. Dean, J. A. "Lange's Handbook of Chemistry," 14th ed. McGraw–Hill, New York, 1992.
12. Fahy, G., and Ali, S. Cryopreservation of the mammalian kidney. II. Demonstration of immediate ex vivo function after introduction and removal of 7.5 M cryoprotectant. *Cryobiology* **35,** 114–131 (1997).
13. Fahy G. M., Levy D. I., and Ali S. E. Some emerging principles underlying the physical properties, biological actions, and utility of vitrification solutions. *Cryobiology* **24,** 114–131 (1997).
14. Fahy G. M., Lilley T. H., Linsdell H., Douglas M. S., and Meryman H. T. Cryoprotectant toxicity and cryoprotectant toxicity reduction: In search of molecular mechanisms. *Cryobiology* **27,** 247–268 (1990).
15. Fahy, G., MacFarlane, D., Angell, C., and Meryman, H. Vitrification as an approach to cryopreservation. *Cryobiology* **21,** 407–426 (1984).
16. Hagedorn M., Hsu E., Kleinhans F. W., and Wildt D. E. New approaches for studying the permeability of fish embryos: Toward successful cryopreservation. *Cryobiology* **34,** 335–347 (1997).
17. Karow, A. Cryoprotectants—A new class of drugs. *J. Pharm. Pharmacol.* **21,** 209–223 (1969).
18. MacFarlane, D. R. Devitrification in glass-forming aqueous solutions. *Cryobiology* **23,** 230–244 (1986).
19. MacFarlane, D. R. Physical aspects of vitrification in aqueous solutions. *Cryobiology* **24,** 181–195 (1987).
20. MacFarlane, D. R., and Forsyth, M. Devitrification and recrystallization of glass-forming aqueous solutions. *In* "The Biophysics of Organ Cryopreservation" (D. E. Pegg and A. M. Karow, Eds.), NATO ASI Series, Series A, Life Sciences, Vol. 147, pp. 237–263. Plenum, New York/London, 1987.
21. MacFarlane, D. R., and Fragoulis, M. Theory of devitrification in multi-component glass forming systems under diffusion control. *Phys. Chem. Glasses* **27,** 228–234 (1986).
22. MacFarlane, D. R., Fragoulis, M., Uhlerr, B., and Jay, S. D. Devitrification in aqueous solution glasses at high heating rates. *Cryo-Lett.* **7,** 73–80 (1986).
23. Naccache, P., and Sha'afi, R. I. Patterns of nonelectrolyte permeability in human red blood cell membrane. *J. Gen. Physiol.* **62,** 714–736 (1973).
24. Rasch, C. M., and Wowk, B. Toxicity of glycol ether cryoprotectants in a kidney slice model. *Cryobiology* **37,** 407–408 (1998). [Abstract]
25. Santarius K. A., and Bauer J. Cryopreservation of spinach chloroplast membranes by low-molecular-weight carbohydrates. I. Evidence for cryoprotection by a noncolligative-type mechanism. *Cryobiology* **20,** 83–89 (1983).
26. Schuff-Werner, P., Muller, U., Ungler, C., Nagel, G. A., and Eibl, H. 1-*O*-Methyl-rac-glycerol: A new agent for the cryopreservation of mononuclear cells. *Cryobiology* **25,** 487–494 (1988).
27. Sutton, R. L. Determination of time–temperature transformation and continuous cooling curves for propan-1-2-diol. *Cryo-Lett.* **11,** 49–58 (1990).
28. Sutton, R. L. Critical cooling rates to avoid ice crystallization in solutions of cryoprotective agents. *J. Chem. Soc. Faraday Trans.* **87,** 101–105 (1991).
29. Sutton, R. L. Critical cooling rates for aqueous cryoprotectants in the presence of sugars and polysaccharides. *Cryobiology* **29,** 585–598 (1992).
30. Suzuki, T., Boediono, A., Takagi, M., Saha, S., and Sumantri, C. Fertilization and development of frozen–thawed germinal vesicle bovine oocyte by a one-step dilution method *in vitro*. *Cryobiology* **35,** 515–524 (1996).
31. Takagi, M., Boediono, A., Saha, S., and Suzuki, T. Survival rate of frozen–thawed bovine IVF embryos in relation to exposure time using various cryoprotectants. *Cryobiology* **30,** 306–312 (1993).
32. Takagi, M., Sakonju, I., Otoi, T., Hamana, K., and Suzuki, T. Postthaw viability of the inner cell mass of *in vitro*-matured/*in vitro*-fertilized bovine embryos in various cryoprotectants. *Cryobiology* **31,** 398–405 (1994).
33. Vorotilin. Cryoprotective properties of ethylene glycol ethers during freezing of human erythrocytes. *Kriobiologiya* **3,** 31–34 (1987).
34. Wowk, B., Federowicz, M., Harris, S. B., Rasch, C. M., and Okouchi, Y. Methoxylation of cryoprotectants for vitrification. *Cryobiology* **37,** 407 (1998). [Abstract]